

NASA Out-Year Planning

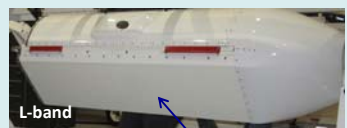
Oct. 20-22, 2015

Oil Observing Tool Workshop

1

UAVSAR

UAVSAR Pod on Gulfstream-III



Antenna can be changed to a different band and still use the common electronics back end:



P-band



Ka-band

- ❖ UAVSAR is an L-band Synthetic Aperture Radar (SAR) developed by NASA to support **repeat-pass radar interferometry** and to also serve as a **radar technology test bed** for future space-borne imaging radar missions.
- ❖ Instrument in the non-pressurized pod is compact, modular, and adaptable to support multiple airborne platforms and frequency upgrades.



Technology

2 complete L-band radars; electronically steered antennas compensate for winds ; G-III precision auto-pilot, 1 m x 1.7 m resolution

Science

L-band repeat-pass InSAR for surface deformation, vegetation structure, soil moisture mapping, land use classification, cryospheric studies, and archaeological research

2

EFFECT OF SURFACE LAYER OF OIL ON RADAR BACKSCATTER FROM WATER

Oil damps the small-scale capillary and gravity-capillary waves on the ocean surface mainly through a reduction in the surface tension at the gas-liquid interface.

Dispersion relationship for waves at the interface between air and a liquid of density ρ with surface tension σ :

$$\rho_{oil}/\rho_{water} \approx 0.8 - 0.9$$

$$\sigma_{oil}/\sigma_{water} \approx 0.25 - 0.5$$

$$\omega^2 = gk + (\sigma/\rho)k^3$$

gravity is the restoring force

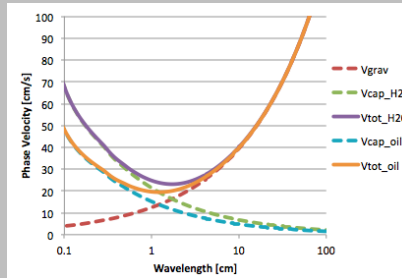
surface tension and inertia are the restoring forces

$$v_{phase} = \sqrt{\frac{g}{k} + \frac{\sigma}{\rho}k}$$

for a given velocity, k increases when the surface tension decreases

Ocean waves are excited by resonant forcing in a turbulent wind field. The wavelength of capillary waves resonantly excited in the presence of oil is smaller than for a clean water-air interface, hence the damping of the smaller wavelengths. This affects the roughness scale of the water surface. In a real slick, the surface characteristics will vary between pure H₂O and pure oil, depending upon layer thickness, oil type, and areal coverage.

Also, in viscoelastic fluids gravity waves with short wavelength are damped by restoring forces arising from gradients in the surface tension (Marangoni effect).



Oil Observing Tool Workshop

BRAGG SCATTERING THEORY

WAVE FACET MODEL

Radar backscatter from the ocean surface is dominated by scattering from small scale capillary and gravity-capillary waves that roughen the surface. In Bragg scattering theory, the dominant mechanism is resonant backscatter from surface waves of wave number k_{Bragg} where

$$k_{Bragg} = 2k \sin(\theta_{inc})$$

$$k = \frac{2\pi}{\lambda_{radar}}$$

As the incidence angle increases, the wavelength of the Bragg surface wave decreases to a minimum of $\lambda_{radar}/2$ at grazing angles.

L-band ($\lambda_{radar}=23.8$ cm) : $\lambda_{Bragg} = 23.8$ cm (30°), 13.7 cm (60°)

$$\sigma_{HH} = 4\pi k^4 \cos^4(\theta_i) W(2k \sin(\theta + \psi), 2k \cos(\theta + \psi) \sin \beta) \left(\frac{\sin(\theta + \psi) \cos \beta}{\sin \theta_i} \right)^2 R_{HH} + \left(\frac{\sin \beta}{\sin \theta_i} \right)^2 R_{VV}^2$$

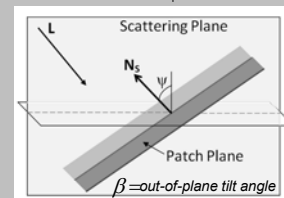
Ocean wave spectral density at Bragg wavelength

$$\sigma_{VV} = 4\pi k^4 \cos^4(\theta_i) W(2k \sin(\theta + \psi), 2k \cos(\theta + \psi) \sin \beta) \left(\frac{\sin(\theta + \psi) \cos \beta}{\sin \theta_i} \right)^2 R_{VV} + \left(\frac{\sin \beta}{\sin \theta_i} \right)^2 R_{HH}^2$$

$$\sigma_{HV} = 4\pi k^4 \cos^4(\theta_i) W(2k \sin(\theta + \psi), 2k \cos(\theta + \psi) \sin \beta) |R_{VV} - R_{HH}|^2$$

$$\theta_i = \cos^{-1}[\cos(\theta + \psi) \cos(\beta)]$$

$$R_{VV} = \frac{(\epsilon_r - 1)(\epsilon_r(1 + \sin^2(\theta)) - \sin^2(\theta))}{(\epsilon_r \cos(\theta) + \sqrt{\epsilon_r - \sin^2(\theta)})^2} \quad R_{HH} = \frac{\epsilon_r - 1}{(\cos(\theta) + \sqrt{\epsilon_r - \sin^2(\theta)})^2}$$



Oil Observing Tool Workshop

POLARIMETRIC DECOMPOSITION

ENTROPY/ANISOTROPY/ALPHA

The Scattering Matrix relates the incident and scattered electric field vectors:

$$\begin{pmatrix} E_H \\ E_V \end{pmatrix}_{scattered} = \begin{pmatrix} S_{HH} & S_{HV} \\ S_{VH} & S_{VV} \end{pmatrix} \begin{pmatrix} E_H \\ E_V \end{pmatrix}_{incident}$$

The scattering matrix is expressed in the Pauli basis as

$$\begin{pmatrix} S_{HH} & S_{HV} \\ S_{VH} & S_{VV} \end{pmatrix} \xrightarrow{Pauli} k = \frac{1}{\sqrt{2}} [S_{HH} + S_{VV} \quad S_{HH} - S_{VV} \quad 2S_{HV}]^T$$

Diagonalization of the coherency matrix $T = k k^*$ gives 3 eigenvalues, λ , and eigenvectors, u . Those define the scattering mechanisms and their backscattered power.

The Cloude-Pottier polarimetric decomposition yields 4 variables derived from the eigenvalues and eigenvectors:

$$\text{Entropy: } H = \sum_{i=1}^3 \left(\frac{\lambda_i}{\lambda_1 + \lambda_2 + \lambda_3} \right) \text{Log}_3 \left(\frac{\lambda_i}{\lambda_1 + \lambda_2 + \lambda_3} \right) \quad 0 \leq H \leq 1$$

$$\text{Anisotropy: } A = \frac{\lambda_2 - \lambda_3}{\lambda_2 + \lambda_3} \quad 0 \leq A \leq 1$$

$$\text{Mean angle: } \bar{\alpha}(u)$$

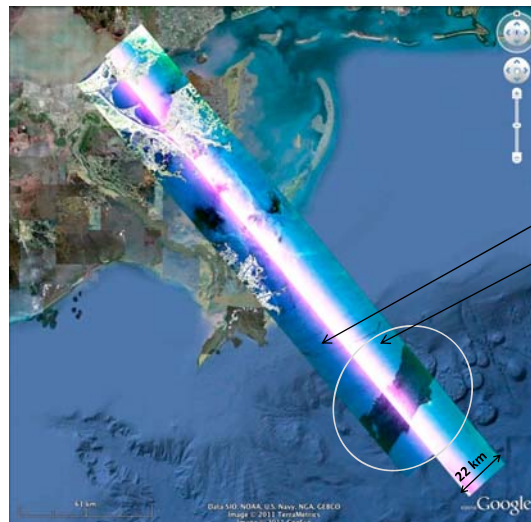
$$\text{Averaged intensity: } \Lambda = \sum_{i=1}^3 \left(\frac{\lambda_i^2}{\lambda_1 + \lambda_2 + \lambda_3} \right)$$

Observing Tool Workshop

5

UAVSAR FLIGHT LINES

THE MAIN SLICK OF THE DEEPWATER HORIZON SPILL



Two UAVSAR lines viewing the main slick from opposite directions were used in our analysis of the polarimetric response of the oil from the DWH spill.

gulfco_32010_10054_101_100623

collected 23-June-2010 21:08 UTC

gulfco_14010_10054_100_100623

collected 23-June-2010 20:42 UTC



Sea state: 1.0-1.3 m SWH
Wind: 2.5-5 m/s from 115°-126°

6

Oil Observing Tool Workshop

NASA's Oil Spill Remote Sensing Relevant Sensors Spaceborne

Instrument (Satellite)	Bands (# bands)	Band Range (nm)	Resolution (km)	Swath (km)	Revisit (days)	Rapid Response	Acronym
MODIS (Terra, Aqua)	Vis, MIR, TIR (36 bands)	405-14,385	0.25,0.5,1.0	2330	1-2	Yes	Moderate Resolution Imaging Spectroradiometer
ASTER (Terra)	VNIR, NIR, TIR (14 bands)	520-11,650	0.015/0.03/0.09	60	4-16	No	Advanced Spaceborne Thermal Emission and Reflection Radiometer
MISR (Terra)	Vis, NIR (4 Bands)	446.4-866.4	0.275-1.1	360	2-9	No	Multiangle Imaging SpectroRadiometer
HICO	Vis-NIR (90 bands)	400-1000	0.95	43	-	No	Hyperspectral Imager for the Coastal Ocean
CALIOP (CALIPSO)	Vis, NIR (2 bands)	532, 1064	0.1	-	16	No	Cloud Aerosol Lidar with Orthogonal Polarization (Cloud-Aerosol Lidar and Infrared Pathfinder Satellite Observation)

Table from: Leifer et al., in *Time Sensitive Remote Sensing*, Lippitt et al. (eds.), Springer, in press
Oil Observing Tool Workshop